Pergamon

Journal of Structural Geology, Vol. 17, No. 9, pp. 1249 to 1265, 1995

0191-8141/95 $9.50+0.00

0191-8141(95)00026-7

# Kinematics of rock flow and the interpretation of geological structures, with particular reference to shear zones

DAZHI JIANG and JOSEPH CLANCY WHITE

Centre for Deformation Studies in the Earth Sciences, Department of Geology,
The University of New Brunswick, Fredericton, NB, Canada E3B 5A3

(*Received* 23 *July* 1994; *accepted in revised form* 15 *February* 1995)

**Abstract**—Current interpretations of structures are generally based on homogeneous and steady deformation models, despite the fact that both the heterogeneity of rocks (materially, rheologically and geometrically) and the time dependence of imposed geological conditions give rise to significant heterogeneous and non-steady flow. In concert with field observations, we emphasize that the expectation of heterogeneity and non-steadiness is the key to understanding natural deformation and that in order to carry out successful structural analysis and tectonic interpretation, it is necessary to recognize the first-order distinction between imposed boundary conditions typically used to define the tectonic regime (e.g. transcurrent, transpression) and the response recorded by rocks within the zone (structures and fabrics). Using S–C fabric as an example, it is demonstrated how flow with a non-zero spinning component resulting from the rheological contrasts and/or geologically realistic time-dependent boundary displacement can drastically change the 'ideal' geometric and kinematic relations between the fabric and the host zone. In agreement with both theoretical analysis and field observation, it is shown that natural flow regimes range from pure shear to pure rotation, including super-simple shear. In consideration of the heterogeneity and non-steadiness of natural deformation, kinematic analysis is justifiable only within a homogeneous domain and steady period. Flow kinematics and mechanisms are interrelated in that, firstly, mechanisms provide internal constraints on kinematics, ensuring that only certain flows are possible and, secondly, flow kinematics will favour development of certain mechanisms.

## INTRODUCTION

Deformation of the earth can be largely organized, for a given scaling dimension, into zones of deformation. At the simplest level, such zones comprise subjectively defined boundaries and an intervening volume of rock which typically exhibits more intense deformation or a higher density of structures than material outside the boundaries. Such descriptions are the result of field observations of deformation localization and heterogeneous finite strain, with the most widely studied examples being characterized as *shear zones* in recognition of displacement dominantly parallel to the zone boundaries. Structural analysis is the mapping and interpretation of heterogeneities (e.g. lithological contrast, folds, foliations, lineations, S–C fabrics, rotated porphyroclasts) within deformed rocks. In the classical works by Sander (1911, 1930, 1948, 1950, 1970) and Turner & Weiss (1963), natural deformation was clearly treated as complex. The seminal work of Ramsay & Graham (1970) stands out as a demonstration of how structures within a shear zone can be related to boundary displacements (Fig. 1a). Using strict assumptions and significant simplification, McKenzie & Jackson (1983) obtained the relationship between strain rates, palaeomagnetism, finite strain and fault movements within a shear zone. Assuming a two-dimensional time-independent Newtonian rheology, Ramberg (1986) showed that flow and the accumulating finite deformation can be elegantly dealt with by the stream function method. These ideal models are all valid within their assumptions and have provided insights into understanding structural and fabric development. However, subsequent structural studies, particularly of shear zones, have often neglected the assumptions behind such models. Over the ensuing years, many geologists have implicitly treated shear zones, irrespective of scale, as having single homogeneous movement pictures when they correlate 'shear-sense indicators' to boundary displacements.

The tendency to rely on 'simple shear' for studies of shear zone deformation is largely due to the statement made by Ramsay & Graham (1970, p. 799) on the basis of strain compatibility which, as cited by Simpson & De Paor (1993, p. 2) states "simple shear is the only constant volume strain regime that can occur in straight, parallel-sided shear zones bounded by undeformed wall rocks". It must be emphasized that this conclusion does not hold unless two additional conditions are met: (1) the deformation throughout the shear zone must be homogeneous, at least in the direction parallel to the shear zone boundary; and (2) the deformation must be continuous. It has been demonstrated that even if boundary conditions are identical to those of Ramsay and Graham shear zones, the deformation within the zone is no longer simple shear if rocks exhibit rheological contrasts (Jiang 1994a) or if discontinuous deformation is involved (Lister & Williams 1979).

Based on both the ubiquitous field evidence for heterogeneous deformation (Fig. 1b) and theoretical investigations (Lister & Williams 1983, Ishii 1992, Jiang 1994a,b), we maintain that expectation of heterogeneity, not search for homogeneity, is the key to understanding natural deformation.

Complex non-steady flow of rock occurs when: (1) the rock is rheologically heterogeneous (Jiang 1994a,b), even if boundary conditions are constant; and/or (2) the boundary conditions vary, even if the rock is rheologically homogeneous. The above encompass virtually every condition relevant to natural deformation. In what follows, we: (1) summarize and develop some of the general principles of natural deformation; (2) investigate the non-steadiness of natural flow as a result of inconstant boundary displacement (non-steadiness resulting from rheological contrasts has been treated elsewhere, Jiang 1994a,b); and (3) demonstrate how spinning flow (typical of general non-steady flow) can change the geometric and kinematic relations between the fabric and the host zone.

## FLOW KINEMATICS—GENERAL STATEMENT

Sander (1911, 1930, 1948, 1950) showed that structures and fabrics can be interpreted in terms of 'movement pictures' on the basis of the symmetry principle (Paterson & Weiss 1961, Turner & Weiss 1963, Lister & Williams 1979, see discussion by Hobbs 1985). Movement picture can be best described by the concepts and terminology of flow (Sander 1970, p. 12) which are well documented in the earth sciences literature (Ramberg 1975, McKenzie 1979, Means *et al.* 1980, Lister & Williams 1983, Hoeppener *et al.* 1983, Passchier 1986, Simpson & De Paor 1993, Jiang 1994a,b, Means 1994). These are summarized briefly in the following.

Deformation-induced flow can be described by the Eulerian gradient tensor (**L**) of the velocity field. Since the gradient of uniform translation is always zero, **L** can be kinematically decomposed into a stretching tensor (**D**) and a vorticity tensor (**W**), i.e. $\mathbf{L} = \mathbf{D} + \mathbf{W}$ (Truesdell 1954, Sedov 1971). The three eigenvalues ($s_1, s_2, s_3$) of **D** are the principal strain rates whose orientations (eigenvectors of **D**) are the three instantaneous stretching axes (ISA). Vorticity is a measure of the rotation rate of material lines with respect to an external frame and is itself decomposable into $\mathbf{W}_S$, a component appropriate for the rotation rate of the ISA in the selected external frame, and $\mathbf{W}_I$, the internal or shear-induced vorticity component (Truesdell 1953, Means *et al.* 1980, Lister & Williams 1983) where $\mathbf{W} = \mathbf{W}_S + \mathbf{W}_I$. Being skew symmetric, a vorticity tensor can be simply expressed by a vector called the vorticity vector whose magnitude is 'the magnitude of vorticity' (denoted by the non-bold $W$ in this paper). For the simple relation between the vector and tensor notations of vorticity, the reader is referred to Means *et al.* (1980) and Passchier (1986). In this paper, we use 'vorticity' in general for both notations.

$\mathbf{W}_S$, whose magnitude equals twice the angular velocity of the ISA, is generally called *spin* (e.g. Means *et al.* 1980, Lister & Williams 1983). Means *et al.* (1980) and Means (1994) used spin as the angular velocity of the ISA, in which case spin is half the magnitude of $\mathbf{W}_S$. In Truesdell & Toupin (1960), and as adopted by Cobbold & Gapais (1987) and Twiss & Moores (1992), spin was used to mean the tensor notation of vorticity, whereas the term 'vorticity' was restricted to the vector notation. We favour the usage of spin as a component of vorticity equal to $\mathbf{W}_S$, as in Lister & Williams (1983, p. 12). Homogeneous flow occurs only when **L** is constant throughout the rock volume. Steady flow occurs when **L** does not change with time.

The intensity of stretching can be described by the effective shear strain rate, $\Gamma$, (cf. Frost & Ashby 1982) where $\Gamma = \{2/3[(s_1 - s_2)^2 + (s_2 - s_3)^2 + (s_3 - s_1)^2]\}^{1/2}$. In isochoric (constant volume) flow, $s_1 + s_2 + s_3 \equiv 0$ and $\Gamma = [2(s_1^2 + s_2^2 + s_3^2)]^{1/2}$. The ratio of the magnitude of total vorticity to effective shear strain rate is Truesdell's kinematic vorticity number ($W_k = W/\Gamma$) and describes the rotational intensity of the flow. The ratio of the magnitude of the internal vorticity to effective shear strain rate defines Means' or the internal kinematic vorticity number ($W_k' = W_I/\Gamma$), which measures the degree of non-coaxiality.

## THE CHARACTERIZATION OF BULK FLOW

### *Boundary conditions vs zone deformation*

The analysis of rock deformation in terms of discrete zones is based on the observation that curviplanar regions of deformation are readily defined during field study. In this context, zonal deformation comprises regions within and outside the zone demarcated by an assigned boundary which collectively form a study area. The choice of such boundaries can be very subjective and has, as an underlying motive, the pragmatic resolution of field geometries and tectonic histories. Geologically, boundaries can be defined variously as tectonostratigraphic discontinuities or lower limits of finite strain that can be recognized or are of interest to a specific study. For large-scale features, boundaries commonly reflect the far-field displacements (tectonic displacements) of the zone host. The imposed effects of the boundary on the intervening material are the *boundary conditions*. For the purpose of kinematic analysis they comprise the geometry, displacement history and migration of the boundary (Means 1984, Jiang 1994a). The response of the intervening material is characterized using the structural geometry, style and intensity of deformation and associated deformation attributes. The latter in turn influences the assignation of geological definitions to the particular zone (e.g. kink band, shear zone, fold belt). This differentiation between zone and boundaries arises from the abundant field evidence for heterogeneous behaviour in the earth and is a basic aspect of field methodology whereby structural domains are established on the basis of variations in geometrical attributes.

It is essential to differentiate between displacements related to the zone boundaries and the response of the intervening rock. In two-dimensional flow cases, the only kinematic connection between boundary displacement (Fig. 5) and the deforming zone is the bulk

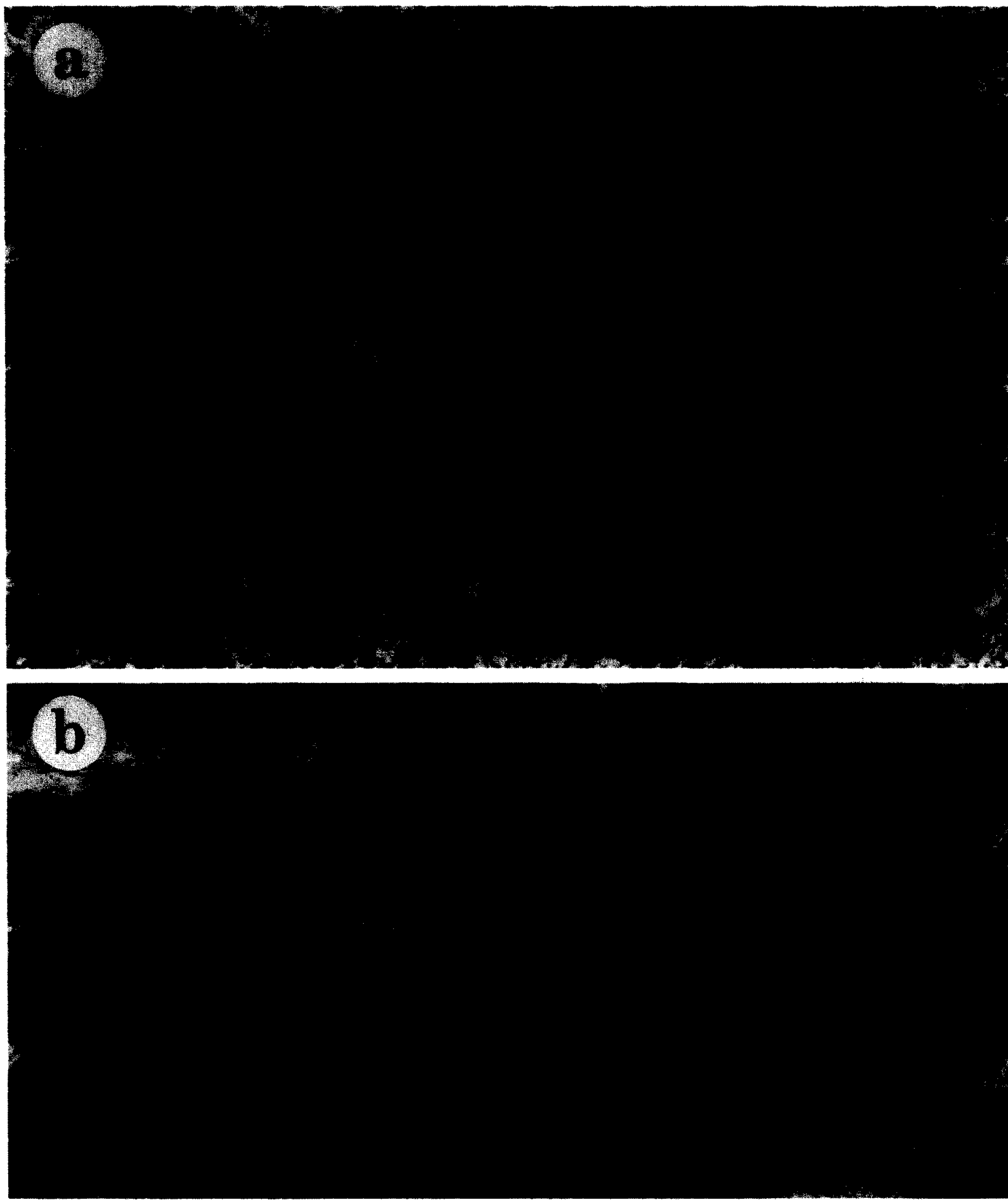


Fig. 1. Natural examples of shear zones. (a) Typical Ramsay & Graham (1970) shear zone, where the boundary displacement, internal finite strain and deformation paths are commonly interpreted to have simple and generally applicable relationships (metagabbro, North Uist, Outer Hebrides, Scotland; scale—2.3 cm diameter coin). Shear zones of larger scale with similarly looking strain gradients may have much more complicated histories (Means in press). (b) Generalized shear zone showing heterogeneous deformation which is necessarily non-steady (Jiang 1994a) (granulite gneiss, Dunchurch, Ontario; scale bar—5 cm).

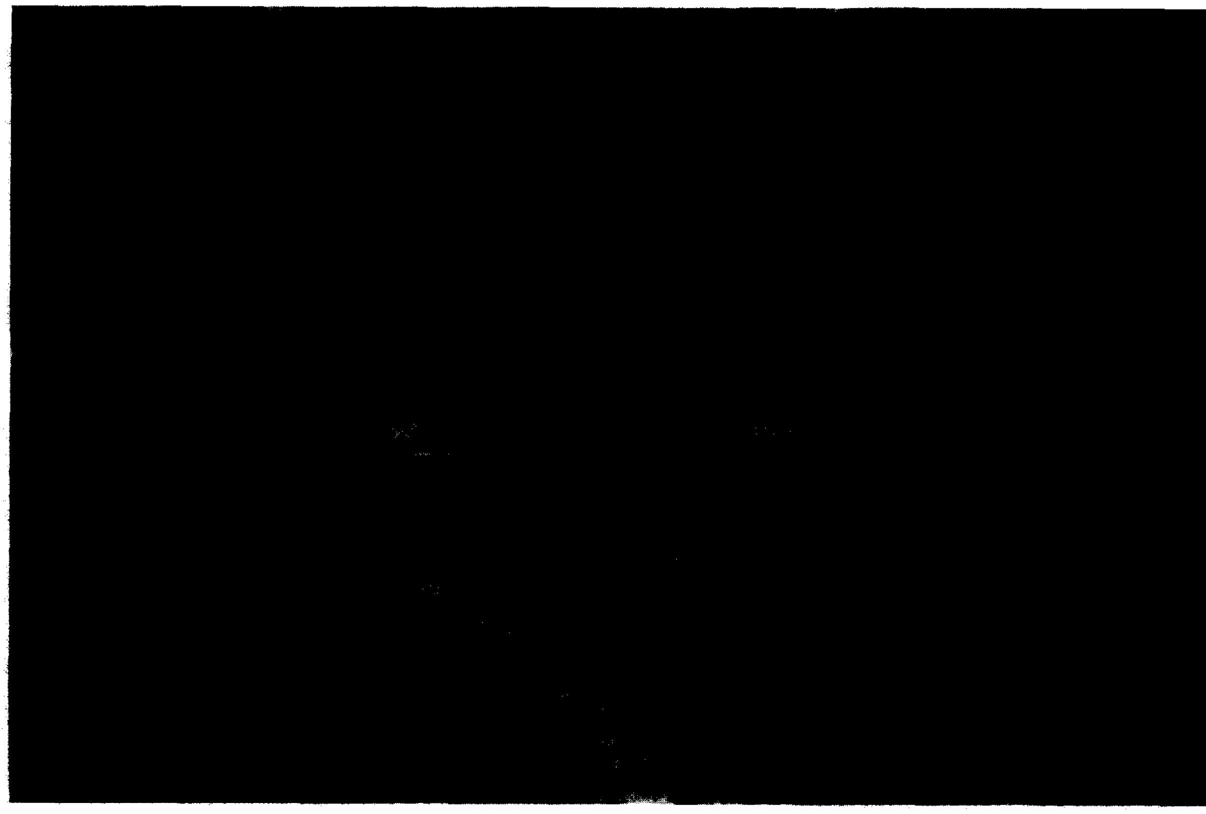

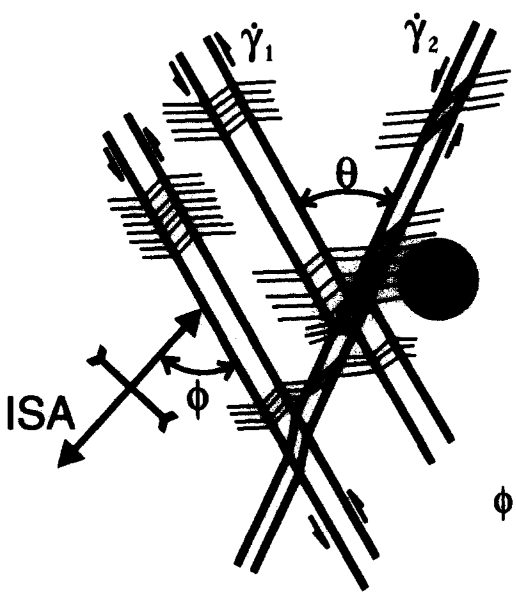


$$C = \dot{\gamma}_1 / \dot{\gamma}_2$$

$$W'_k = \frac{1 + C}{(1 + C^2 + 2C\cos 2\theta)^{1/2}}$$

$$\phi = \tan^{-1} \frac{\sin 2\theta + (1 + C^2 + 2C\cos 2\theta)^{1/2}}{C + \cos 2\theta}$$

Fig. 2. A natural example of super-simple shear where two sets of shear bands develop and cut each other, indicating concurrent development. They are both sinistral. The shear-strain rates accommodated by the two sets as they developed are denoted by $\dot{\gamma}_1$ and $\dot{\gamma}_2$, respectively. $C$ is the ratio of the two shear-strain rates. At any time during the development of the structure, if $C$ was nearly constant, i.e. the spin component of the vorticity was negligible, the internal kinematic vorticity number (non-coaxiality) at that time is greater than unity (see Appendix for detail). Equal development of the two bands suggests that $C \approx 1$. This gives $W'_k = 1.74$. See text and Appendix for details. Huronian metasedimentary rocks, Espanola, Ontario; scale—6 cm diameter lens cap.

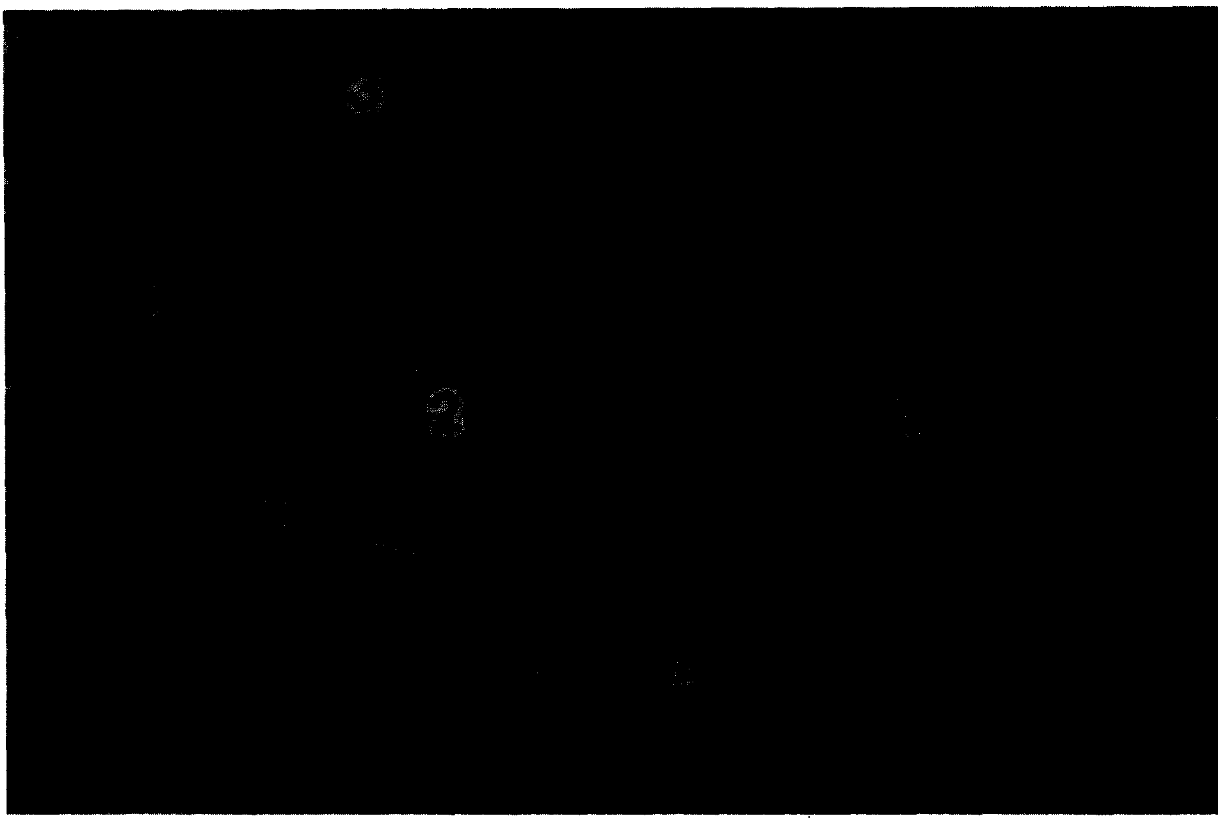

Fig. 3. Kinematic indicators in a porphyroclast-rich (perthite and hornblende) gneiss from the Parry Sound shear zone, Dunchurch, Ontario. The bulk shear zone boundary is parallel to horizontal edges of the photograph. S-planes are defined by shape fabrics (porphyroclast shape) and C-planes are defined by compositional layering. S is initially oblique to C (1), but as finite strain accumulates, S rotates toward C which acts as a sink for material lines. At high finite strain (2), S and C are parallel and cannot be differentiated. Compositional layering in such rocks is characteristically the product of high finite strain and defines a kinematically-initiated shear band (C-plane). Shear bands formed in this way tend to have diffuse boundaries. Kinematically-initiated shear bands can develop in any orientation relative to the shear zone boundaries (3) as an inherent attribute of heterogeneous and non-steady flow. Subsequently, kinematically-initiated shear bands can be used as sites for strain localization (4 shows progressive development from left to right) leading to development of mechanically-initiated shear bands (5) which are characterized by discrete boundaries. On the other hand, mechanically-initiated shear bands may, with increasing finite strain, rotate towards the sink parallel to kinematically-initiated shear bands, precluding differentiation of the two. Scale bar—5 cm.

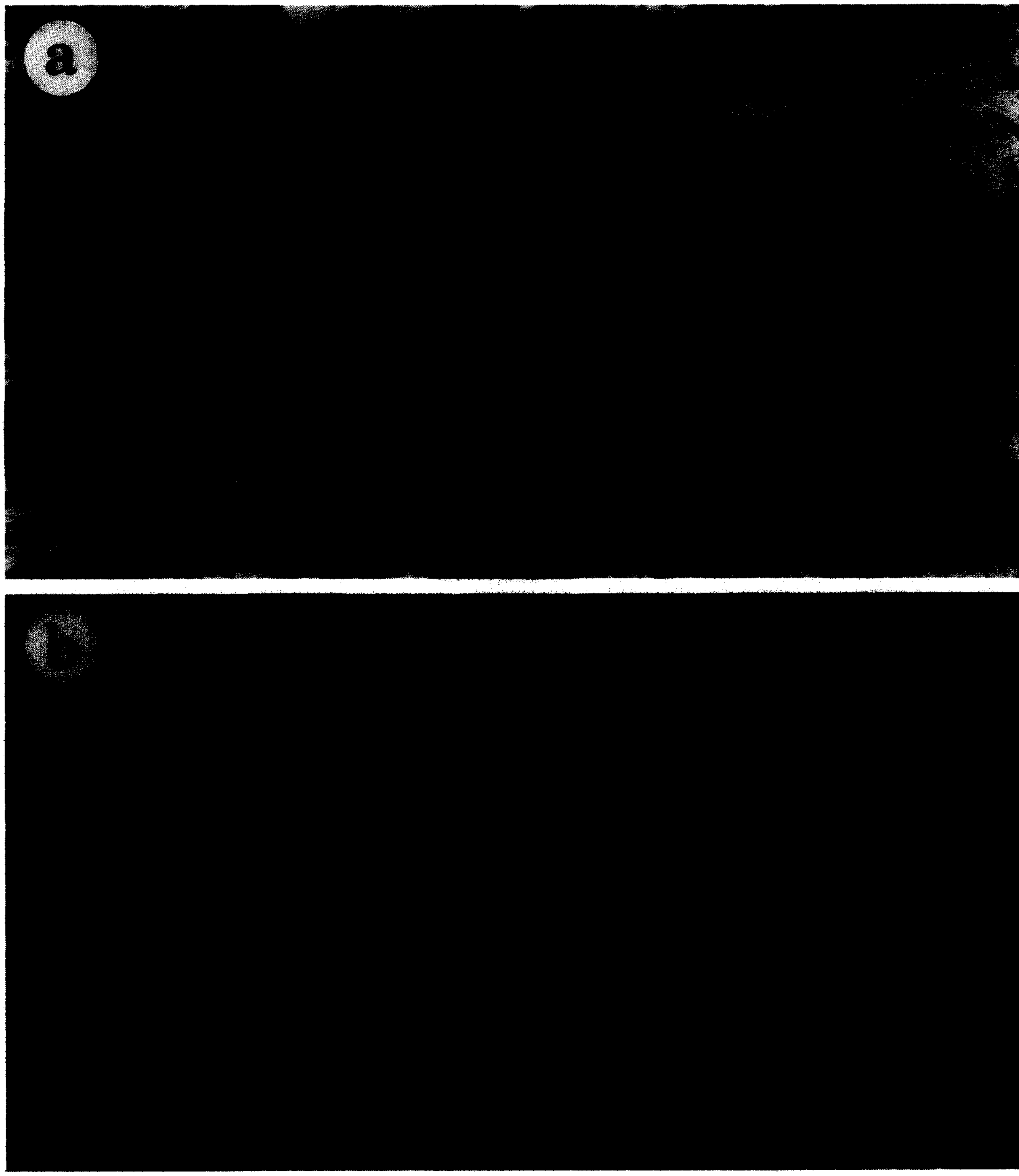

Fig. 4. Strain paths recorded by rocks can be strongly influenced by available deformation mechanisms. In particular, the distribution and partitioning of vorticity among different lithologies can be largely determined by the most economical combination of kinematic path and micromechanical behaviour. (a) Calcite mylonite with 'non-coaxial' fabric reflecting activity of dislocation glide and dynamic recrystallization (amphibolite-grade shear zone, Maniwaki, Quebec; scale bar—100 $\mu$m). (b) Carbonate–quartz-mica rock with extensive 'flow folding' producing sheath folds that reflect the dominance of grain-size-sensitive flow mechanisms in this fine-grained (<10 $\mu$m) material (sub-greenschist-grade shear zone, Cobequid fault zone, Nova Scotia; scale bar—5 cm).

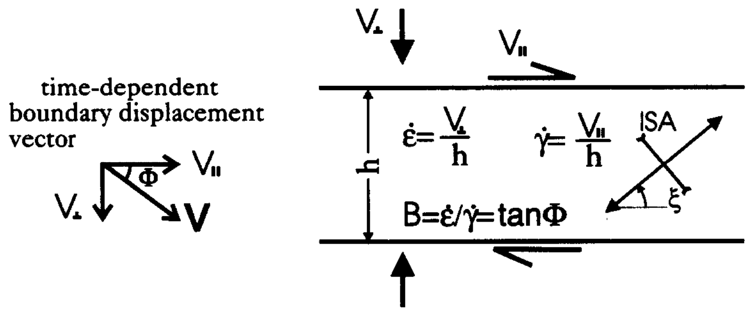


Fig. 5. Boundary conditions vs internal deformation. Boundary conditions (geometry, displacement and migration) set up the instantaneous bulk vorticity which can be ascribed to a time-dependent boundary displacement vector (e.g. a plate velocity). Bulk, instantaneous deformation can be defined in terms of shear strain rate ($\dot{\gamma}$) and stretching (shortening) strain rate ($\dot{\varepsilon}$) normal to the shear zone. These are analogous to the commonly used 'pure shear' and 'simple shear' components of the deformation. Either rheological heterogeneity or inconstant boundary displacement ($\mathrm{d}B/\mathrm{d}t \neq 0$) will give rise to the spinning of the ISA of the flow in the zone. The development of structures and fabrics within the zone depends on such flows.

vorticity, $\mathbf{W}_\mathbf{b}$, (the vorticity averaged over the whole deformation area at any instant, see Jiang 1994a). Even given knowledge of the boundary displacements, which will set up the bulk vorticity, it has been explicitly demonstrated (Jiang 1994a) that *the nature of the imposed bulk vorticity (boundary displacements) does not constrain the kinematics of structures within the deforming zone.*

*The ubiquity of non-steady deformation*

In the vector sense, boundary displacements can be expected to be a function of time during natural deformation. This means both the magnitude and/or orientation of boundary velocities can vary with time and position along the boundary. We now present a simple demonstration of how non-steady displacement of a shear zone boundary can induce complex bulk flow, even in rheologically homogeneous rocks. The reference frame for this and subsequent discussions is fixed to the zone boundaries (Fig. 5). We will only consider plane isochoric flow with the bulk vorticity axis perpendicular to the plane (i.e. flow with monoclinic symmetry). The method can be easily applied to such transpressional/transtensional models as Fossen & Tikoff (1993) and Tikoff & Teyssier (1994), but this is considered redundant for this study.

Consider a general oblique boundary displacement vector making an angle of Φ with respect to the shear zone boundary. The displacement-rate vector (**v**) can be resolved into a boundary-parallel ($v_\parallel$) and a boundary-normal ($v_\perp$) component. Using $h$ to denote the instantaneous width of the shear zone, the bulk shear strain rate ($\dot{\gamma}$) and bulk stretching (or shortening) rate ($\dot{\varepsilon}$) normal to the shear zone boundary are, respectively (Fig. 5):

$$\dot{\gamma} = \frac{v_\parallel}{h} \qquad (1)$$
$$\dot{\varepsilon} = \frac{v_\perp}{h}.$$

The velocity gradient tensor of the bulk flow is (see Ramberg 1975):

$$\mathbf{L} = \begin{bmatrix} \dot{\varepsilon} & \dot{\gamma} \\ 0 & -\dot{\varepsilon} \end{bmatrix}. \qquad (2)$$

Since the boundary displacement is time dependent, both $\dot{\varepsilon}$ and $\dot{\gamma}$ will be functions of time.

The magnitude of the bulk vorticity, $W_\mathrm{b}$, measured in this reference frame simply equals the bulk shear-strain rate, $\dot{\gamma}$. The intensity of the rotational component of the flow measured in this frame is given by the Truesdell's kinematic vorticity number $W_\mathrm{k}$, which can be reformulated as:

$$W_\mathrm{k} = [(2\dot{\varepsilon}/\dot{\gamma})^2 + 1]^{-1/2}. \qquad (3)$$

If the boundary displacement rate is non-steady, $W_\mathrm{k}$ will be time-dependent.

The maximum ISA makes an angle $\xi$ with respect to the shear zone boundary giving (Fig. 5):

$$\xi = \tan^{-1}\frac{1 - \sqrt{1 - W_\mathrm{k}^2}}{W_\mathrm{k}} = \frac{1}{2}\sin^{-1}W_\mathrm{k}$$
$$= \tan^{-1}[(1 + 4B^2)^{1/2} - 2B], \qquad (4)$$

where $B = \dot{\varepsilon}/\dot{\gamma}$ can vary over time; that is, velocities both parallel and normal to the zone are allowed to vary over time. The magnitude of spin ($W_\mathrm{S}$) is given by:

$$W_\mathrm{S} = \mathrm{spin} = -2\frac{\mathrm{d}\xi}{\mathrm{d}t} = \frac{2}{1 + 4B^2}\frac{\mathrm{d}B}{\mathrm{d}t} = \frac{\mathrm{d}}{\mathrm{d}t}\cos^{-1}W_\mathrm{k}. \qquad (5)$$

The negative sign indicates that the reduction of $\xi$ corresponds to sympathetic spin, i.e. having the same sense as the bulk vorticity.

The magnitude of the internal or shear-induced vorticity ($W_\mathrm{I}$) and internal kinematic vorticity ($W'_\mathrm{k}$), the measure of non-coaxiality, are respectively:

$$W_\mathrm{I} = \dot{\gamma} - W_\mathrm{S} \qquad (6)$$

and

$$W'_\mathrm{k} = \frac{\dot{\gamma} - W_\mathrm{S}}{(4\dot{\varepsilon}^2 + \dot{\gamma}^2)^{1/2}}. \qquad (7)$$

When $W_\mathrm{S} > \dot{\gamma}$, i.e. $W'_\mathrm{k} < 0$, the sense of non-coaxiality of the flow is the reverse of that imposed by the boundary displacement shear sense. This requires:

$$\frac{dB}{dt} > \frac{1 + 4B^2}{2}\dot{\gamma} \quad (8)$$

which is satisfied when $d\Phi/dt > 2\dot{\gamma}$.

When $W'_k > 1$, bulk scale super-simple shear (De Paor 1983) occurs. This requires that:

$$\frac{dB}{dt} < \frac{1 + 4B^2}{2}\dot{\gamma}[1 - (1 + 4B^2)^{1/2}]$$

which can be reformulated as:

$$\frac{d\Phi}{dt} < 0, \qquad \text{and}$$
$$\left|\frac{d\Phi}{dt}\right| > 2\dot{\gamma}[(1 + 4\tan^2\Phi)^2 - 1]. \quad (9)$$

For a natural shear-strain rate of $10^{-14}\,s^{-1}$, a reverse sense of non-coaxiality occurs for a variation of the boundary displacement vector at a rate of $3.6 \times 10^{-5}$ degree $y^{-1}$. Similarly, if the displacement vector is initially at 45° to the shear zone boundary, bulk-scale super-simple shear occurs if the orientation decreases at a rate of $4.5 \times 10^{-5}$ degree $y^{-1}$.

The size of the boundary of a deformation depends on the scale of interest. On the scale of plate boundaries, long-lived (1 Ma), monotonic variation of the displacement vector on the order of $10^{-5}$ degree $y^{-1}$ appears rare, although fluctuations about some mean vector are not precluded. Observations of natural deformation strongly suggest that the smaller the scale, the more inconstant the boundary. On the scale of a fold limb, during the time period of fold development, the boundary displacement vector imposed by the adjacent layers may vary as much as 90°, if the fold develops toward being isoclinal. Commonly observed successive refolding (e.g. Bell 1978, Cobbold & Quinquis 1980, Hudleston 1989) in ductile shear zones estimated to span a time period on the order of one million years (see Pfiffner & Ramsay 1982 and references therein) suggests that the variation of the boundary displacement vector on, or greater than, the order of $10^{-5}$ degree $y^{-1}$ is easily achieved on the outcrop scale. It is at this scale where essentially all direct studies of structures, observation and data collecting are practised. Therefore, we conclude that super-simple shear and reverse sense of non-coaxiality are to be expected at the map-scale. When considering the kinematic history of a deformation, it is necessary to anticipate non-steady flow histories with the possibility of reverse non-coaxiality and flow regimes ranging over pure shear, sub-simple shear, simple shear and super-simple shear.

## DEFORMATION PATH AND STRUCTURES

### *Deformation paths: kinematics and mechanism*

Understanding a path requires knowledge of the evolution with time of some state in the vicinity of a material point. For structural studies, such a vicinity can be viewed as a parametrically homogeneous domain whose size depends on the scale of interest and the complexity of structures. Metamorphic studies routinely consider such paths, where pressure and temperature define the state, and evolution with time gives a *P–T–t* path.

Kinematically, the flow state at a point can be completely characterized by three *kinematic numbers*: $W_k$, $W'_k$ and $A_k$, the kinematic dilatancy number—a measure of volume change rate (Passchier 1991a, cf. Jiang 1994b). Plotting these three parameters in $W_k$–$W'_k$–$A_k$ space and chaining the points by the time arrow will define the *kinematic path* ($W_k$–$W'_k$–$A_k$–$t$ path) for that vicinity. Mechanistically, deformation is achieved by certain mechanisms whose time history defines the mechanism-*t* path. Kinematic and mechanistic paths define the *deformation path*. There is both expectation and observational support for spatial variation of deformation paths, and it has been theoretically demonstrated that in rocks with layers of varied competence, each layer will follow a different kinematic path (Ishii 1992, Jiang 1994b). The deformation paths of all the domains, i.e. the distribution of deformation paths, depict the whole movement picture. The relationship between $W_k$, $W'_k$ and the competence factors of the layers, and their time behaviour, for isochoric flow, are shown in fig. 9 of Jiang (1994b), from which a $W_k$–$W'_k$–$A_k$–$t$ path can be constructed. However, the deformation paths of natural deformation remain difficult to establish, although attempts have been made since at least the beginning of this century (Sander 1911, Flinn 1962, Elliott 1972, Ramsay & Wood 1973, Passchier & Urai 1988, Vissers 1989, Passchier 1990, and reviews by Wenk & Christie 1991, Means 1994). Some difficulties and associated problems that must be acknowledged during interpretations of field data are briefly discussed in the following.

### *The nature of structural records*

"Something of the origin and evolution of any rock is recorded in its fabric" (Turner & Weiss 1963, p. 36).

Structures or fabrics generally can only record an incomplete history—something rather than everything—of the deformation. This is because: (1) the rock record is temporally discontinuous—structures, fabrics and kinematic indicators strictly speaking can record one or several, but rarely all deformation increments; and (2) rocks commonly exhibit fading memory—they tend to forget their remote past experience (Hobbs 1972, Ferguson 1979, Means 1989, Passchier *et al.* 1990, White & Flagler 1992). Transposition and recrystallization are two ways amongst others by which rocks lose their record of the remote past. In the case of a steady-state fabric (Means 1981), the rocks only record their latest flow state. As a result of this incompleteness of structural records, correlation of different deformation domains must be done carefully (Williams 1985).

Also, most structures and fabrics need not show a unique correspondence to the deformation path. For example, shortened or folded boudins can be interpreted as the result of at least four different types of deformation paths: (1) steady super-simple shear (Means *et al.* 1980, Hanmer & Passchier 1991); (2) overprinting of a later shortening on an earlier extension; (3) volume change (von Brunn & Talbot 1986); and (4) non-steady flow (Jiang 1994a). Unless sufficient independent constraints are available, uniqueness is not achievable (Hudleston & Lan 1993).

*Distribution, partitioning and the dilemma with the estimate of spin*

Lister & Williams (1983) used the term *partitioning* to mean: (1) the kinematic decomposition of the velocity field and especially the decomposition of vorticity into internal or shear-induced vorticity and spin components; and (2) spatial variation of a quantity like strain, strain rate or vorticity. Ramsay & Huber (1983, p. 113) have used the term mechanistically to mean the separation of the total deformation into various contributing mechanisms such as pressure solution, grain boundary sliding and crystal plastic strain. Means (personal communication) has pointed out that mechanistic partitioning is always a matter of spatial partitioning, e.g. crystal plastic strain within the grains and grain boundary sliding in the regions between grains. In a recent paper by Mohanty & Ramsay (1994), partitioning has been used to mean the factorization (Ramsay & Huber 1987, p. 838, Means 1994) of the finite strain into volume change, heterogeneous simple shear etc. Lister & Williams' dual meaning of the term is the most commonly used (e.g. Hanmer & Passchier 1991, Ishii 1992, Simpson & De Paor 1993). For clarity, Jiang (1994a) has restricted the term *partitioning* to the *kinematic decomposition at a point* of a quantity such as vorticity. *Distribution* has been formally introduced to mean the *spatial variation* of a quantity. Familiar examples of distribution include the gradient of a shear strain, which may also indicate a distribution of shear-strain rate, across a Ramsay and Graham shear zone and the variations in finite strain among different structural domains (e.g. Wood 1973, Ramsay 1982, Paterson *et al.* 1989, Stauffer & Lewry 1993, Goodwin & Wenk in press).

Once partitioning and distribution of flow are clearly differentiated, it can be recognized that spin is not simply the variation in orientation of a marker line such as bedding. In a simple natural fold, we may be able to estimate the rotation of the layer if we know its prefolding attitude, but this provides no information regarding the spin of the ISA in the layer unless the deformation path is assumed. What we can hope to derive from the symmetry of the structures or fabrics is non-coaxiality (Sander 1970, Means *et al.* 1980, Passchier 1990, Means 1994). A train of asymmetric folds or a fabric with monoclinic symmetry is commonly attributed to non-coaxial flow. However, such attributes are internal (domainal) and say nothing about the spin of the ISA in that domain with respect to an external frame. Although there is no effective way to estimate the spin history, spin is kinematically important because (1) it will change the magnitude and/or even sense of $W_k'$ which is directly related to the symmetry of the structures and fabrics, and (2) spin will change the orientations of flow eigendirections and, therefore, the geometric relationship between the structures and the host zone. In practice, spin is often implicitly set at zero. This has created an unnecessary dilemma for structural interpretations.

*Super-simple shear*

McKenzie (1979) considered super-simple shear ($W_k' > 1$, De Paor 1983) to be the most common flow type in mantle circulation rather than simple shear ($W_k' = 1$). Such flow has distinct implications for structure and mixing in the mantle (Allègre & Turcotte 1986, Turcotte 1991). However, in crustal deformation, simple shear and pure shear are routinely treated as the upper and lower limits of natural flow (Pfiffner & Ramsay 1982, Passchier 1990, Hanmer & Passchier 1991), whereas super-simple shear is considered to be possible only at the grain-scale (Means 1981, Talbot & Jackson 1987) or in the vicinity of deformable porphyroclasts (Simpson & De Paor 1993). Jiang (1994a,b) has theoretically demonstrated that even in bulk sub-simple shear ($0 < W_k' < 1$) environments, super-simple shear flow can occur as a result of rheological contrasts. Additionally, we have demonstrated above that geologically realistic boundary inconstancy can induce super-simple shear. Therefore, the preclusion of super-simple shear has no theoretical foundation. The difficulty in identifying super-simple shear in rocks may be a reason for such a state. Current methods to estimate non-coaxiality will preclude super-simple shear because they require that the ISA be irrotational with respect to the shear zone boundary, ensuring that the shear zone boundary is always a flow eigenvector. In so doing, the flow can never have a kinematic vorticity number exceeding 1.

The structure in Fig. 2 demonstrates a super-simple shear regime. Two sets of shear bands are developed in metasedimentary rocks. They cut each other, indicating concurrent development, and have the same sinistral sense of shear. No matter what the shear-strain rates accommodated by the two bands are and irrespective of whether they were time-dependent, as long as their ratio is nearly constant, the internal kinematic vorticity (non-coaxiality) for the simultaneous development of the two sets is always greater than unity (Fig. 2, see Appendix for the formulation of $W_k'$).

Since both stretching and vorticity contribute to finite deformation (Mitra 1976, McKenzie 1979), the degree of non-coaxiality is also a measure of the efficiency of finite strain accumulation (Pfiffner & Ramsay 1982) during flow. Pfiffner & Ramsay (1982) demonstrated that it is impossible to estimate the strain rate of natural deformation using finite strain markers without presuming the deformation path. As the existence of super-simple shear will put different constraints on the available paths, its influence on such calculations requires discussion. Pfiffner & Ramsay (1982) consider simple shear ($W'_k = 1$) as the most inefficient flow and pure shear ($W'_k = 0$) as the most efficient flow for the accumulation of uniform finite strain in nature and obtained natural strain rates in the range of $10^{-12}$ to $10^{-15}$ s$^{-1}$. If super-simple shear is taken into consideration, the most inefficient flow should be pure rotation ($W'_k = \infty$). In such a case, the actual natural strain rate can be much higher because the observed finite strain will require a higher strain rate to achieve within the estimated time period if a much less efficient path ($W'_k > 1$) was taken. Strain rate within a particular structural domain is itself not a prescribed parameter, but will depend on boundary movement rate and deformation distribution (White & Mawer 1992).

## DEVELOPMENT OF KINEMATIC INDICATORS—SHEAR-BAND CLEAVAGE AND TAILED PORPHYROCLASTS

### *Kinematic and mechanical shear bands*

Foliations in ductile shear zones are ubiquitously sought out as kinematic indicators (e.g. Platt & Vissers 1980, Simpson & Schmid 1983, Platt 1984, Weijermars & Rondeel 1984, Hanmer 1986, Passchier 1991b, Hanmer & Passchier 1991). We use them as examples to demonstrate the effect of spinning flow. The theoretical considerations can be similarly applied to other indicators such as rotated porphyroclasts (Passchier & Simpson 1986).

The two types of cleavage recognized are S cleavage (schistosity) and shear-band cleavage (Berthé *et al.* 1979, Jégouzo 1980, Ponce de Leon & Choukroune 1980, Platt & Vissers 1980, Lister & Snoke 1984, Harris & Cobbold 1984, Dennis & Secor 1987, 1990). In the literature, shear-band cleavages parallel or subparallel to the host shear zone boundary have been termed C-planes, whereas those oblique to the host shear zone boundary have been variously termed as shear band cleavage (White 1979, White *et al.* 1980), asymmetrical extensional crenulation cleavage (Platt & Vissers 1980), C′-bands (Ponce de Leon & Choukroune 1980) and normal slip crenulation (Dennis & Secor 1990). In contrast to this complex nomenclature, Lister & Snoke (1984) did not make any differentiation among shear band cleavages merely on their orientations, probably in recognition that they are often microstructurally indifferentiable. Lister & Snoke (1984, fig. 9) and especially Behrmann (1987) emphasized that shear band cleavage may have different geometric and kinematic relationships with respect to the shear zone boundary. We adopt this broad definition of the S–C fabric.

Foliations ascribed to shear band cleavage can have both a kinematical and mechanical origin. The kinematical origin is related to the alignment of material lines (e.g. mica traces) along, and the progressive rotation of shape fabrics such as the S-foliation toward the flow extensional eigenvector. This origin usually occurs in relatively pervasive plastic deformation and the shear bands often have diffuse boundaries. The orientation of such shear bands is solely controlled by flow kinematics. An excellent example is found in fig. 1 of Simpson & Schmid (1983), where C foliation is clearly a result of large finite strain. The mechanical origin is related to shear strain localization that forms yield surfaces, in which case, the developing shear band cleavages serve as new deformation mechanisms which often overprint earlier foliations (e.g. S foliation, earlier shear bands). The orientation of such shear bands is determined by the interaction between the orientations of the principal stresses and rock anisotropy. Figure 5 of Simpson & Schmid (1983) demonstrates this, where the shear-band cleavage is more localized, discrete and has relatively well defined boundaries, which overprints shape fabrics. We wish to emphasize that once a shear-band cleavage is initiated, irrespective of its origin, the subsequent development can be complex, particularly when the associated deformation conditions (e.g. pressure, temperature, strain rate) change. For example, kinematically-initiated shear bands may subsequently serve as sites of strain localization and become geometrically analogous to Riedel shears (see Bartlett *et al.* 1981, Shimamoto 1989). Similarly, mechanically-initiated shear bands of various orientation may become parallel to the flow eigenvector as finite strain accumulates. The recognition of two types of shear-band cleavage emphasizes the need to clearly distinguish between geometry and genetics.

Mechanical initiation of shear bands has been studied experimentally by Shimamoto (1989) and Williams & Price (1990). Results have provided insights into mylonites and cataclasites in shear zones (Shimamoto 1989, Babaie *et al.* 1991). In the following, we investigate the kinematical initiation that typically occurs under more pervasive plastic deformation conditions. We demonstrate that shear-band cleavage developed in this way can have various geometric and kinematic relations with the host shear zone as a result of spinning flow histories.

### *Orientations and sense of non-coaxiality of shear bands*

It is clear from the partitioning of flow that the description of a flow is different in different reference frames if these frames rotate, one with respect to another. For example, the flow description within a shear zone can be represented by different Eulerian velocity gradient tensors such as $\mathbf{L}_{SZB}$ or $\mathbf{L}_{ISA}$ depending on whether the shear zone boundary (SZB) or the ISA are taken as the reference frame. The kinematic vorticity number of $\mathbf{L}_{SZB}$, $W_k$, is always $\leq 1$ and the SZB is always an eigenvector of $\mathbf{L}_{SZB}$ (extensional or contractional depending on whether the shear zone is a narrowing one or widening one, see Simpson & De Paor 1993). Whereas $\mathbf{L}_{ISA}$ is directly related to the fabric, $\mathbf{L}_{SZB}$ is not. The kinematic vorticity number of $\mathbf{L}_{ISA}$, $W'_k$, is the non-coaxiality. Unlike $W_k$, $W'_k$ can be greater than one, in which case no eigenvectors exist in the plane perpendicular to the vorticity vector. If $W'_k \leq 1$, the eigenvec-

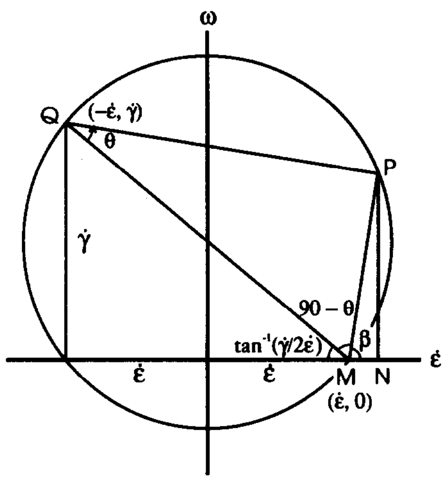


$$QM = (4\dot{\varepsilon}^2 + \dot{\gamma}^2)^{1/2}$$

$$PM = QM \sin\theta$$

$$\beta = 180 - (90 - \theta) - \tan^{-1}(\dot{\gamma}/2\dot{\varepsilon})$$
$$= 90 + \theta - \tan^{-1}(\dot{\gamma}/2\dot{\varepsilon})$$

$$\omega = PN = PM \sin\beta$$
$$= \dot{\gamma}\sin^2\theta + \dot{\varepsilon}\sin 2\theta$$

Fig. 6. Mohr circle construction for determining the instantaneous angular velocity of material lines with respect to the reference frame fixed to the shear zone boundary (Fig. 5). M and Q are plots of the shear zone boundary and shear zone normal, respectively. An arbitrary material line making an angle $\theta$ with respect to the shear zone boundary is plotted at P. Its angular velocity $\omega$ is the length of PN, which is perpendicular to the horizontal axis.

tors of $L_{ISA}$ can be obtained by finding the orientation(s) of the material line(s) having the same angular velocities as the spin of the ISA, i.e.:

$$2\omega = \text{spin} \qquad (10)$$

where $\omega$ is the angular velocity of material lines.

In the bulk flow field described in equations (1)–(9), the angular velocity ($\omega$) of a material line making an angle $\theta$ with respect to the shear zone boundary can be obtained from the Mohr circle construction (Fig. 6) where:

$$\omega = \dot{\gamma}\sin^2\theta + \dot{\varepsilon}\sin 2\theta \qquad (11)$$

Incorporating (3)–(11) and after manipulation, the particular angles ($\theta_c$) for (10) to hold are:

$$\theta_c = \frac{\pm\cos^{-1} W'_k - \cos^{-1} W_k}{2}. \qquad (12)$$

Although in the chosen reference frame $W_k$ is always $\leqslant 1$, $W'_k$ can exceed 1, as has been demonstrated (equation 9).

When $W'_k > 1$, $\theta_c$ does not exist because the flow is super-simple shear characterized by no material line being irrotational with respect to the ISA.

When $W'_k = 1$, the flow is simple shear, and one eigenvector exists with $\theta_c = -1/2\cos^{-1}W_k$.

When $0 \leqslant |W'_k| < 1$, the flow is sub-simple shear, and two $\theta_c$ exist.

When $W'_k = 0$, the flow is pure shear, two $\theta_c$ exist and coincide with the two principal strain-rate axes.

It is now clear that time-dependent boundary displacement will result in spin, as will rheological contrasts (Jiang 1994b). Depending on the sense and rate of spin ($W_S$), flow varies over the range of pure shear to super-simple shear. The rotation intensity and flow non-coaxiality can be represented by Mohr circles. Figure 7 explicitly shows that fabrics are not only related to the sense and magnitude of non-coaxiality (Means *et al.* 1980), but are also related to spin, in that spin changes both the non-coaxiality and the orientation of eigendirections. It is this spin that can give rise to the various observed geometric and kinematic relationships of structures and fabrics to their host shear zone boundaries. We demonstrate this using the development of S–C fabrics as an example (Fig. 8). The principles elucidated can be similarly applied to any other kinematic indicators such as rotated porphyroclasts.

*Case I*: *spin* $= 0$

This type of bulk flow occurs when either: (1) the boundary displacement rate is steady; or (2) the ratio of boundary-normal longitudinal strain rate to the boundary-parallel shear-strain rate is constant (i.e. $B = \dot{\varepsilon}/\dot{\gamma} = \text{constant}$). In both cases, $W_k = W'_k$ and the angle between the extensional eigenvector of $L_{ISA}$ and the shear zone boundary ($\theta$) is zero. This represents the implicitly assumed condition for all existing shear zone interpretations. The direction parallel to the shear zone boundary is a sink of all material lines and a shear-band cleavage will develop parallel to it. In this case, C-planes must be parallel to the shear zone boundary and the sense of non-coaxiality of the S–C fabric does indicate the sense of boundary displacement.

*Case II*: *spin* $> 0$ *but* $0 < W'_k < W_k$

The situation for spin $> 0$ occurs when either the convergent component of displacement grows or the divergent component decays at a rate faster than the transcurrent component. When the induced spin is not strong enough to result in reverse non-coaxiality, we have $\theta < \xi$. In this case, the C fabric will make an angle to the shear zone boundary, but the sense of non-coaxiality is the same as the sense of boundary displacement. This is commonly observed in the field where C-planes are subparallel to or deviate a few tens of degrees from the host shear zone boundary (e.g. Goodwin & Wenk in press).

*Case III*: *spin* $> 0$ *and* $W'_k < 0$, *reverse sense of non-coaxiality*

This situation occurs under the same boundary conditions as case II, but spin is strong enough to induce a reverse sense of non-coaxiality, i.e. $W'_k < 0$. In this case $\theta > \xi$, and not only is the C fabric not parallel to the shear zone boundary, but the sense of non-coaxiality is

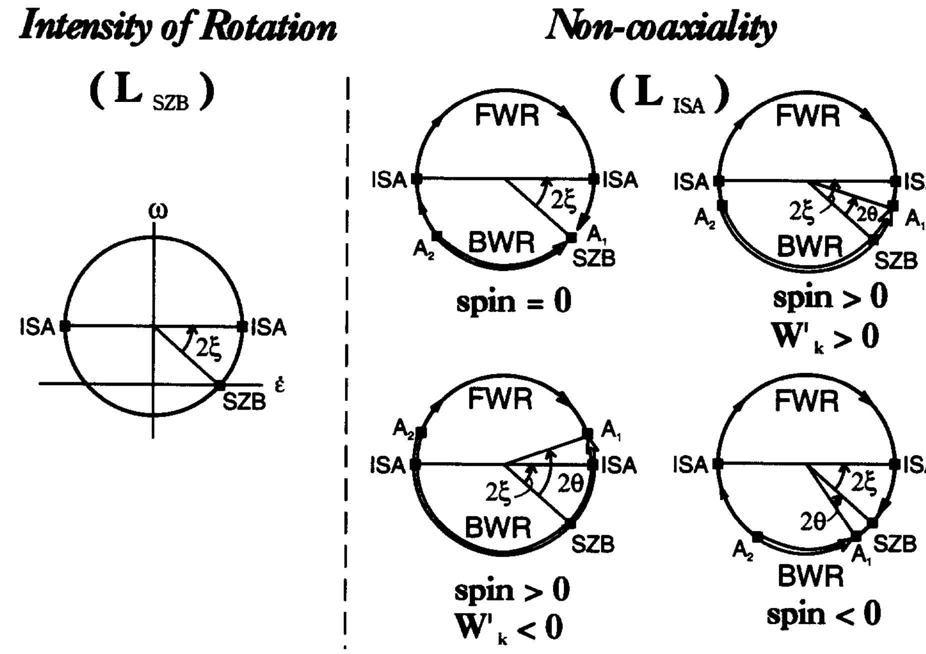


Fig. 7. Mohr circles demonstrating the fundamental difference between the intensity of rotation ($W_k$) and degree of non-coaxiality ($W_k'$). Since the external reference frame is selected to be pinned to the shear zone boundary (Fig. 5), the shear zone boundary (SZB) is always *irrotational* in such a frame. Non-coaxiality ($W_k'$) describes the rotation properties of material lines with respect to the ISA. In this internal reference frame, the SZB rotates except when spin = 0. Depending on the sense and rate of the spin, the two eigenvectors of the flow examined in the ISA frame ($A_1$, extensional and $A_2$, contractional) make different angles ($\theta$) with the SZB, and the sense of non-coaxiality may vary. Material lines having forward (FWR) and backward (BWR) rotation relative to the bulk shear sense can be represented for different flow states.

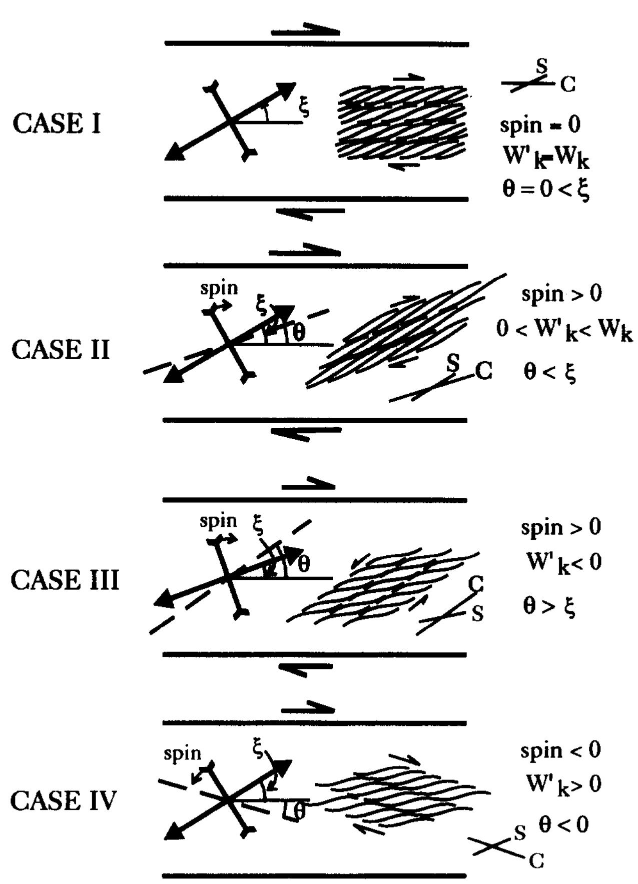


Fig. 8. The kinematic and geometric relationships of S–C fabrics to the host shear zone can vary significantly as a result of the spin of the ISA. Since only the extensional eigenvector (dashed line) is the stable end orientation of material lines (cf. Ghosh & Ramberg 1976), the contractional eigenvector of the flow is not indicated. See text for detail.

antithetic to the boundary displacement. For such fabrics to develop, equation (8) has to be satisfied. As already discussed, this may not be feasible on a plate scale, but such variations are not precluded at the mapping scale. Figure 2 of Behrmann (1987) is an excellent example of this case.

*Case IV: spin* $< 0$

The boundary condition for this case is opposite to that of cases II and III in that $W_k'$ always exceeds $W_k$. In this case, transcurrent velocity components grow faster than the convergent components, or *vice versa*, the transcurrent velocity decays more slowly than the convergent component. When spin is strong enough, bulk super-simple shear ($W_k' > 1$) will occur, in which case only a S fabric is expected to develop, because there are no end orientations for material lines. When $Wk \leqslant 1$, $\theta < 0°$, what are denoted as S–C′ or C–C′ fabrics will develop. Figure 35(b) of Hanmer & Passchier (1991) is an example of this case.

The above demonstration explicitly shows that kinematically-initiated shear-band cleavages can have any orientations relative to the host shear zone boundary. Therefore, the rigid classification of shear-band cleavages into C- and C′-planes solely on their orientation is inappropriate. This emphasizes the correctness of Lister & Snoke (1984) in not linking S–C fabrics with any orientation relative to the host shear zone. Non-steadiness of flow derived from either boundary inconstancy or rheological contrasts removes any requirement that the local flow eigenvector and tectonic transport direction be equivalent. Thus, the S–C fabric can have complex geometric and kinematic relations to the host shear zones. Clearly, any assumptions of correspondence between local shear-band cleavage (C-planes) and boundary displacements appropriate to tectonic transport require substantiation in the field. Additionally, the complex development of kinematically- or mechanically-initiated shear-band cleavages as bulk finite strain accumulates may make differences between them indiscernible. The observation of shear-band cleavages forming by two mechanisms is simply a manifestation of distribution and partitioning of flow at the observed scale.

Porphyroclasts and associated foliations (tails and wings) can have equally complex geometric relationships (Fig. 3); the latter is anticipated given that non-steady flow must occur in the presence of rheological heterogeneities. Stauffer & Lewry (1993) describe excellent examples of variably oriented winged porphyroclasts ascribed to 'general non-coaxial flow' (Hanmer & Passchier 1991, Simpson & De Paor 1993). Finite strain gradients (fig. 2 of Stauffer & Lewry 1993) result from strain distribution on a large scale, while a wide variety and orientation of rotated, tailed porphyroclasts develops in response to local variations in non-coaxiality and eigen-directions within specific structural domains (fig. 8 of Stauffer & Lewry 1993).

It is important during interpretations of kinematic indicators to recognize that 'natural variations' do not reflect failure on the part of rock to attain some ideal state, but rather indicate the inherent complexity of the flow that enables structures to develop and from which can be extracted a host of information. It is also important to emphasize that variations in eigen-directions do not develop in response to the relative amounts of transcurrent and convergent displacements, but rather are products of the *relative rates of change* in such displacements.

## DISCUSSION

### *Natural deformation conditions and kinematic analysis*

Structures and fabrics have been related to flow and/or deformation eigen-directions (Hoeppener *et al.* 1983, Bobyarchik 1986, Simpson & De Paor 1993 and this study). In the situation of homogeneous and steady flow, this is simple and straightforward, because these eigen-directions are constant in space and with time. For heterogeneous and non-steady flows, eigen-directions change in space and with time. Flow can be considered approximately homogeneous only within a homogeneous domain. Structures and fabrics will only have a local significance. Hasty correlation of structures or fabrics to distant boundary displacement is not justified.

Compared to the spatial variation (heterogeneity) of natural deformation, variation of natural flow with time (non-steadiness) is even more difficult to deal with. This is because: (1) very few geological criteria exist for linking structures and fabrics to absolute time and for establishing spatial correlation; and (2) with the exception of perhaps steady-state fabrics, a fabric does not generally indicate whether or not, and to what extent, the flow was steady during its development. Means (1976, in press) highlights the problem of relating the spatial variation in strain to rock history of progressive deformation and raises the point that the lower strain portion of a rock volume or body need not represent the earlier stage in the history of the more strained portion. This is because they may have witnessed entirely different kinematical and mechanistic paths and/or metamorphic conditions. As pointed out by Newman & Mitra (1994), the dangers involved can be lessened by using cross-cutting relationships in addition to spatial variation. Geochronology can potentially constrain the time of the deformational fabrics and events (e.g. Gromet 1991, Scott *et al.* 1993), and can sometimes allow evaluation and comparison of the ages of deformational events from different portions of an outcrop, from outcrop to outcrop, and from region to region (Getty & Gromet 1992). This ideally can provide some information regarding the variation of flow distribution with time. However, the resolution of such techniques is only fine enough to distinguish separate deformational events, whereas it is still unable to unravel the processes during a specific event within which a fabric develops. At this stage, there seems no reliable way to evaluate the steadiness of flow during the development of a fabric.

Theoretically, a non-steady flow history may, within prescribed limits, be divisible into several relatively *steady periods*. Only within a steady period can flow eigen-directions be considered approximately constant in orientation. The estimates and ensuing interpretations of the degree of non-coaxiality and/or volume change rate from deformed rocks (Passchier & Urai 1988, Vissers 1989, Passchier 1990, Wallis 1992, see review by Means 1994) are valid only for the homogeneous domain and in the time period during which flow is assumed to be steady.

The previous discussion leads to a conclusion that *kinematic analysis is justified only within a homogeneous domain and a steady period*. The points are summarized in Fig. 9. The bulk vorticity, *Wb* for any prescribed volume of rock, such as a shear zone, can be heterogeneously distributed throughout domains, with further partitioning of the distributed vorticity possible within each domain. Ramifications of such distribution and partitioning include the generation of heterogeneous finite strain and geometrically contrasting, mappable structural domains which cannot be attributed to ideal simple shear. Although it may be demonstrable through mapping that the bulk zone has a 'simple' movement picture (Lister & Williams 1979), the anticipation of complex flow within the zone allows for coherent interpretation of variable structures that are precluded or considered abnormal by the strict application of simple shear or steady sub-simple shear at all scales of observation (see also Robin & Cruden 1994).

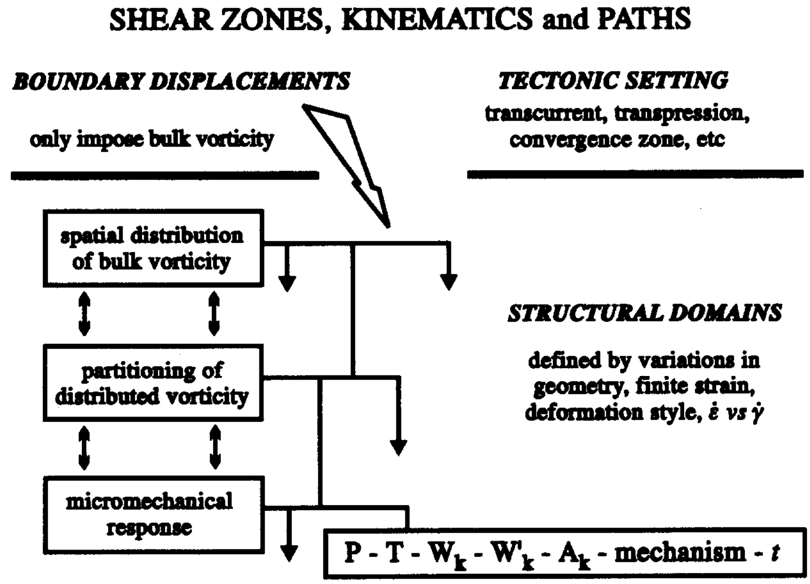


Fig. 9. Schematic illustration of the relationships between concepts of kinematic flow and mapping nomenclature and methodology. Boundary displacements, which are typically used to categorize the type of shear zone, only set up the bulk vorticity within the shear zone. Bulk vorticity can be both spatially distributed and kinematically partitioned throughout the shear zone in response to heterogeneous and non-steady flow. Both distribution and partitioning are interrelated with deformation mechanisms. The spatial variations of parameters resulting from distribution and partitioning form the basis for mappable structural domains. These domains interact with one another, which is why heterogeneous deformation is often non-steady, leading to temporal and spatial evolution of structures. A primary attribute of such interaction, when coupled with the interdependence of what are commonly considered independent parameters, is that metamorphic, kinematic and mechanistic paths cannot be *a priori* considered in isolation.

*What tells the rock which path to take?*

From the point of view of pure kinematics, there is an infinite variety of paths for a certain finite deformation. However, all such paths are not equivalent dynamically. Dynamic laws will require a volume of rock to follow certain paths. These include balance of mass, balance of linear and angular momentum, conservation of energy, non-negative entropy production and so on (Truesdell & Toupin 1960, Prigogine 1967, Glansdorff & Prigogine 1971). In the simplest situation where mechanical and thermal processes are decoupled, the paths of deformation will be such that the rate of dissipation of energy is maximum or minimum depending on whether the boundary of the deformation is a constant force boundary or a constant velocity boundary (Ramberg 1981, p. 211, 1986). However, there is little to suggest the decoupling of mechanical and thermal processes during natural deformation. To the contrary, it has long been realized that rock deformation cannot be separated from other geological processes such as metamorphism (Zwart 1969, Spry 1969).

At any instant of rock transformation, the kinematic state of the flowing rock, the active deformation mechanisms, metamorphic reactions and dynamic recrystallization etc. define the response of the rock system to the interaction between rock heterogeneity and the conditions imposed by the surrounding rocks (immediate boundary). This response is governed by both the thermodynamic and mechanical laws.

Kinematics and mechanisms are interrelated. On the one hand, the operative mechanisms which determine the rheological response of the rock provide 'internal constraints' (cf. Truesdell 1977) on the kinematics, ensuring that only certain flows are possible. On the other hand, distributed flow in a domain will favour initiation of certain mechanisms. Figure 4 demonstrates the influence different mechanisms can have on the resultant kinematic path.

## CONCLUSIONS

(1) Natural deformation is inherently heterogeneous and non-steady. The development of structures depends on the occurrence of such flow, and interpretation of their genesis and kinematic significance should be made with this in mind.

(2) When zones of deformation are defined by mapping, behaviour of the zone boundaries and intervening rock must be differentiated. The boundary conditions only set up the bulk vorticity but do not constrain the internal deformation. The latter is a function of the distribution of the bulk flow and partitioning of the distributed flow in each domain. The kinematic relationship between boundaries and the intervening rock must be demonstrated rather than assumed.

(3) The classical field discrimination of structural domains using geometrical elements reflects the distribution and partitioning of bulk flow into parametrical domains. Kinematic analysis is justifiable only within a homogeneous domain and a steady period. Integration and comparison of the different domains and periods allow synthesis of larger scale movement pictures.

(4) Dynamic laws will require a volume of rock to follow a certain metamorphism–kinematic–mechanism path compatible with the boundary conditions. This in effect reduces the infinite number of paths based purely on kinematics and may explain the commonly reproduced patterns of deformation that enable successful field mapping.

*Acknowledgements*—We thank Dr Win Means for sending us reprints of his papers and inspiring discussion. Frequent discussion with our UNB colleagues and graduate students, particularly Paul Williams, Jim Ryan, Jüergen Kraus and Peter Stringer have contributed to clarification of ideas herein. We thank Jüergen Kraus for help with German translations. Review comments from Drs P. J. Hudleston and A. Cruden were instructive. Dr Cruden is also thanked for bringing to our attention Ramberg (1986). Review comments by Dr D. G. De Paor urged us to explain certain points especially the description of flow in different reference frames. This study is supported by NSERC Research (A8512) and LITHOPROBE University Supporting Geoscience grants to J. C. White. This is a LITHOPROBE Publication No. 641.

## REFERENCES


Allègre, C. J. & Turcotte, D. L. 1986. Implications of a two-component marble-cake mantle. *Nature* **323**, 123–127.

Babaie, H. A., Baba, A. & Hadizadeh, J. 1991. Initiation of cataclastic flow and development of cataclastic foliation in nonporous quartzites from a natural fault zone. *Tectonophysics* **200**, 67–77.

Bartlett, W. L., Friedman, M. & Logan, J. M. 1981. Experimental folding and faulting of rocks under confining pressure, Part IX, wrench faults in limestone layers. *Tectonophysics* **79**, 255–277.

Behrmann, J. 1987. A precautionary note on shear bands as kinematic indicators. *J. Struct. Geol.* **9**, 659–666.

Bell, T. H. 1978. Progressive deformation and reorientation of fold axes in a ductile mylonite zone: the Woodroffe thrust. *Tectonophysics* **44**, 285–320.

Berthé, D., Choukroune, P. & Jégouzo, P. 1979. Orthogneiss, mylonite and non-coaxial deformation of granites: the example of the South Armorican Shear Zone. *J. Struct. Geol.* **1**, 31–42.

Bobyarchik, A. R. 1986. The eigenvalues of steady state flow in Mohr space. *Tectonophysics* **122**, 35–51.

Cobbold, P. R. & Gapais, D. 1987. Shear criteria in rocks: an introductory review. *J. Struct. Geol.* **9**, 521–523.

Cobbold, P. R. & Quinquis, H. 1980. Development of sheath folds in shear regimes. *J. Struct. Geol.* **2**, 119–126.

Dennis, A. J. & Secor, D. T. 1987. A model for the development of crenulations in shear zones with applications from the Southern Appalachian Piedmont. *J. Struct. Geol.* **9**, 809–817.

Dennis, A. J. & Secor, D. T. 1990. On resolving shear direction in foliated rocks deformed by simple shear. *Bull. geol. Soc. Am.* **102**, 1257–1267.

De Paor, D. G. 1983. Orthographic analysis of geological structures—I. Deformation theory. *J. Struct. Geol.* **5**, 255–278.

Elliott, D. 1972. Deformation paths in structural geology. *Bull. geol. Soc. Am.* **83**, 2621–2638.

Ferguson, C. C. 1979. The simple fluid with fading memory as a rheological model for steady-state flow of rocks. In: *Mechanics of Deformation and Fracture* (edited by Easterling, K. E.). Pergamon, 371–383.

Flinn, D. 1962. On folding during three-dimensional progressive deformation. *Q.J. geol. Soc. Lond.* **118**, 385–433.

Fossen, H. & Tikoff, B. 1993. The deformation matrix for simultaneous simple shearing, pure shearing and volume change, and its application to transpression–transtension tectonics. *J. Struct. Geol.* **15**, 413–422.

Frost, H. J. & Ashby, M. F. 1982. *Deformation-Mechanism Maps. The Plasticity and Creep of Metals and Ceramics*. Pergamon Press, Oxford.

Getty, S. R. & Gromet, L. P. 1992. Geochronological constraints on ductile deformation, crustal extension, and doming about a basement-cover boundary, New England Appalachians. *Am. J. Sci.* **292**, 359–397.

Ghosh, S. K. and Ramberg, H. 1976. Reorientation of inclusions by combination of pure shear and simple shear. *Tectonophysics* **34**, 1–70.

Glansdorff, P. & Prigogine, I. 1971. *Thermodynamic Theory of Structure, Stability and Fluctuations*. Wiley Interscience, London.

Goodwin, L. B. & Wenk, H.-R. In press. Development of phyllonite from granodiorite: mechanisms of grain-size reduction in the Santa Rosa mylonite zone, California. *J. Struct. Geol.*

Gromet, L. P. 1991. Direct dating of deformational fabrics. In: *MAC Short Course on Radiogenic Isotope Systems*. Vol. 19 (edited by Heaman, L. & Ludden, J. N.). Toronto, May, 1991, 167–189.

Hanmer, S. 1986. Asymmetric pull-aparts and foliation fish as kinematic indicators. *J. Struct. Geol.* **8**, 111–122.

Hanmer, S. & Passchier, C. W. 1991. Shear-sense indicators: a review. *Geol. Surv. Can. Pap.* **90–17**.

Harris, L. B. & Cobbold, P. R. 1984. Development of conjugate shear bands during bulk simple shearing. *J. Struct. Geol.* **7**, 37–44.

Hobbs, B. E. 1972. Deformation of non-Newtonian materials in simple shear. In: *Flow and Fracture of Rocks* (edited by Heard, H. C., Borg, I. Y., Carter, N. L. & Raleigh, C. B.). *Am. Geophys. Un., Geophysical Monograph* **16**, 243–258.

Hobbs, B. E. 1985. The geological significance of microfabric analysis. In: *Preferred Orientation in Deformed Metals and Rocks: An Introduction to Modern Texture Analysis* (edited by H.-R. Wenk). Academic Press, Orlando, 463–494.

Hoeppener, R., Brix, M. & Vollbrecht, A. 1983. Some aspects on the origin of fold-type fabrics—theory, experiments and field applications. *Geol. Rdsch.* **72**, 1167–1196.

Hudleston, P. J. 1989. The association of folds and veins in shear zones. *J. Struct. Geol.* **11**, 949–957.

Hudleston, P. J. & Lan, L. 1993. Information from fold shapes. *J. Struct. Geol.* **15**, 253–264.

Ishii, K. 1992. Partitioning of non-coaxiality in deformed rock masses. *Tectonophysics* **210**, 33–43.

Jégouzo, P. 1980. The South Armorican Shear zone. *J. Struct. Geol.* **2**, 39–47.

Jiang, D. 1994a. Vorticity determination, distribution, partitioning and the heterogeneity and non-steadiness of natural deformations. *J. Struct. Geol.* **16**, 121–130.

Jiang, D. 1994b. Flow variation in layered rocks subjected to bulk flow of various kinematic vorticities: theory and geological implications. *J. Struct. Geol.* **16**, 1159–1172.

Lister, G. S. & Snoke, A. W. 1984. S–C mylonites. *J. Struct. Geol.* **6**, 617–638.

Lister, G. S. & Williams, P. F. 1979. Fabric development in shear zones: theoretical controls and observed phenomena. *J. Struct. Geol.* **1**, 283–297.

Lister, G. S. & Williams, P. F. 1983. The partitioning of deformation in flowing rock masses. *Tectonophysics* **92**, 1–33.

McKenzie, D. 1979. Finite deformation during fluid flow. *Geophys. J. R. astr. Soc.* **58**, 689–715.

McKenzie, D. & Jackson, J. 1983. The relationship between strain rates, crustal thickening, palaeomagnetism, finite strain and fault movements within a deforming zone. *Earth & Planet. Sci. Lett.* **65**, 182–202.

Means, W. D. 1976. *Stress and Strain*. Springer, Heidelberg.

Means, W. D. 1981. The concept of steady-state foliation. *Tectonophysics* **78**, 179–199.

Means, W. D. 1984. Shear zones of Type I and II and their significance for reconstruction of rock history. *Geol. Soc. Am. Northeastern Section Meeting Abs.* **16**, 50.

Means, W. D. 1989. Synkinematic microscopy of transparent polycrystals. *J. Struct. Geol.* **11**, 163–174.

Means, W. D. 1994. Rotational quantities in homogeneous flow and the development of small-scale structures. *J. Struct. Geol.* **16**, 437–445.

Means, W. D. In press. Shear zones and rock history. *Tectonophysics*.

Means, W. D., Hobbs, B. E., Lister, G. S. & Williams, P. F. 1980. Vorticity and non-coaxiality in progressive deformations. *J. Struct. Geol.* **2**, 371–378.

Mitra, S. 1976. A quantitative study of deformation mechanisms and finite strain in quartzites. *Contr. Miner. Petrol.* **59**, 203–226.

Mohanty, S. & Ramsay, J. G. 1994. Strain partitioning in ductile shear zones: an example from a Lower Pennine nappe of Switzerland. *J. Struct. Geol.* **16**, 663–676.

Newman, J. & Mitra, G. 1994. Fluid-influenced deformation and recrystallization of dolomite at low temperatures along a natural fault zone, Mountain City window, Tennessee. *Bull. geol. Soc. Am.* **106**, 1267–1280.

Passchier, C. W. 1986. Flow in natural shear zones—the consequences of spinning flow regimes. *Earth & Planet. Sci. Lett.* **77**, 70–80.

Passchier, C. W. 1990. Reconstruction of deformation and flow parameters from deformed vein sets. *Tectonophysics* **180**, 185–199.

Passchier, C. W. 1991a. The classification of dilatant flow types. *J. Struct. Geol.* **13**, 101–104.
Passchier, C. W. 1991b. Geometric constraints on the development of shear bands in rocks. *Geologie Mijnb.* **70**, 203–211.
Passchier, C. W., Myer, J. S. & Kröner, A. 1990. *Field Geology of High-Grade Gneiss Terrains*. Springer-Verlag, Berlin.
Passchier, C. W. & Simpson, C. 1986. Porphyroclast systems as kinematic indicators. *J. Struct. Geol.* **8**, 831–844.
Passchier, C. W. & Urai, J. L. 1988. Vorticity and strain analysis using Mohr diagrams. *J. Struct. Geol.* **10**, 755–763.
Paterson, M. S. & Weiss, L. E. 1961. Symmetry concepts in the structural analysis of deformed rocks. *Bull. geol. Soc. Am.* **72**, 841–882.
Paterson, S. R., Tobisch, O. T. & Bhattacharyya, T. 1989. Regional, structural and strain analysis of terranes in the Western Metamorphic Belt, Central Sierra Nevada, California, *J. Struct. Geol.* **11**, 255–273.
Pfiffner, O. A. & Ramsay, J. G. 1982. Constraints on geological strain rates: arguments from finite strain states of naturally deformed rocks. *J. geophys. Res.* **87**, 311–321.
Platt, J. P. 1984. Secondary cleavages in ductile shear zones. *J. Struct. Geol.* **6**, 439–442.
Platt, J. P. & Vissers, R. L. M. 1980. Extensional structures in anisotropic rocks. *J. Struct. Geol.* **2**, 397–410.
Ponce de Leon, M. I. & Choukroune, P. 1980. Shear zones in the Iberian Arc. *J. Struct. Geol.* **2**, 63–68.
Prigogine, I. 1967. *Introduction to Thermodynamics of Irreversible Processes*. Interscience Publishers, New York.
Ramberg, H. 1975. Particle paths, displacement and progressive strain applicable to rocks. *Tectonophysics* **28**, 1–37.
Ramberg, H. 1981. *Gravity, Deformation and the Earth's Crust*. Academic Press, London.
Ramberg, H. 1986. The stream function and Gauss' principle of least constraint: two useful concepts for structural geology. *Tectonophysics* **131**, 205–246.
Ramsay, J. G. 1982. Rock ductility and its influence on the development of tectonic structures in mountain belts. In: *Mountain Building Processes* (edited by Hsü, K. J.). Academic Press, London, 111–127.
Ramsay, J. G. & Graham, R. H. 1970. Strain variation in shear belts. *Can. J. Earth Sci.* **7**, 786–813.
Ramsay, J. G. & Huber, M. I. 1983. *The Techniques of Modern Structural Geology, Volume* 1: *Strain Analysis*. Academic Press, London.
Ramsay, J. G. & Huber, M. I. 1987. *The Techniques of Modern Structural Geology, Volume* 2: *Folds and Fractures*. Academic Press, London.
Ramsay, J. G. & Wood, D. S. 1973. The geometric effects of volume changes during deformation processes. *Tectonophysics* **16**, 263–277.
Robin, P.-Y. F. & Cruden, A. R. 1994. Strain and vorticity patterns in ideally ductile transpression zones. *J. Struct. Geol.* **16**, 447–466.
Sander, B. 1911. Über Zusammenhänge zwischen Teilbewegung und Gefüge in Gesteinen. *Tschermaks Mineral. Petrol. Mitt.* **30**, 381–384.
Sander, B. 1930. *Gefügekunde der Gesteine*. Springer, Vienna.
Sander, B. 1948. *Einführung in die Gefügekunde der Geologischen Körper. Vol. 1*. Springer, Vienna.
Sander, B. 1950. *Einführung in die Gefügekunde der Geologischen Körper. Vol. 2*. Springer, Vienna.
Sander, B. 1970. *An Introduction to the Study of Fabrics of Geological Bodies* (English edition). Pergamon Press, Oxford.
Scott, D. J., Machado, N., Hanmer, S. & Gariépy, C. 1993. Dating ductile deformation using U–Pb geochronology: examples from the Gilbert River Belt, Grenville Province, Labrador, Canada. *Can. J. Earth Sic.* **30**, 1458–1469.
Sedov, L. I. 1971. *A Course in Continuum Mechanics, Volume* 1, *Basic Equations and Analytical Techniques*. Wolter-Noordhoff, Groningen.
Shimamoto, T. 1989. The origin of S–C mylonites and a new fault zone model. *J. Struct. Geol.* **11**, 51–64.
Simpson, C. & De Paor, D. G. 1993. Strain and kinematic analysis in general shear zones. *J. Struct. Geol.* **15**, 1–20.
Simpson, C. & Schmid, S. M. 1983. An evaluation of criteria to deduce the sense of movement in sheared rocks. *Bull. geol. Soc. Am.* **94**, 1281–1288.
Spry, A. 1969. *Metamorphic Textures*. Pergamon Press, Oxford.
Stauffer, M. R. & Lewry, J. F. 1993. Regional setting and kinematic features of the Needle Falls Shear Zone, Trans-Hudson Orogen. *Can. J. Earth Sci.* **30**, 1338–1354.
Talbot, C. J. & Jackson, M. A. 1987. Internal kinematics of salt diapirs. *Bull. Am. Ass. Petrol. Geol.* **71**, 1068–1098.
Tikoff, B. & Teyssier, C. 1994. Strain modeling of displacement-field partitioning in transpression orogens. *J. Struct. Geol.* **16**, 1575–1588.
Truesdell, C. A. 1953. Two measures of vorticity. *J. Rational Mech. Anal.* **2**, 173–217.
Truesdell, C. A. 1954. *The Kinematics of Vorticity*. Indiana University Press, Bloomington.
Truesdell, C. A. 1977. *A First Course in Rational Continuum Mechanics*. Academic Press, New York.
Truesdell, C. A. & Toupin, R. A. 1960. The classic field theories. In: *Encyclopedia of Physics (edited by Flügge, S.) Volume III: Principles of classical mechanics and field theory*. Springer-Verlag, Berlin, 226–793.
Turcotte, D. L. 1991. Nonlinear dynamics of crust and mantle. In: *Nonlinear Dynamics, Chaos and Fractals* (edited by Middleton, G. V.). *Geol. Assoc. Can. Short Course Notes* **9**, 151–184.
Turner, F. J. & Weiss, L. E. 1963. *Structural Analysis of Metamorphic Tectonites*. McGraw-Hill, New York.
Twiss, R. J. & Moores, E. M. 1992. *Structural Geology*. W. H. Freeman, New York.
Vissers, R. L. M. 1989. Asymmetric quartz *c*-axis fabrics and flow vorticity: a study using rotated garnets. *J. Struct. Geol.* **11**, 231–244.
von Brunn, V. & Talbot, C. J. 1986. Formation of subglacial intrusive clastic sheets in the Dwyka formation of northern Natal, South Africa. *J. sedim. Petrol.* **56**, 35–44.
Wallis, S. R. 1992. Vorticity analysis in a metachert from the Sanbagawa Belt, SW Japan. *J. Struct. Geol.* **14**, 271–280.
Weijermars, R. & Rondeel, H. E. 1984. Shear band foliation as an indicator of sense of shear: field observations in central Spain. *Geology* **12**, 603–606.
Wenk, H.-R. & Christie, J. M. 1991. Comments on the interpretation of deformation tectonites in rocks. *J. Struct. Geol.* **13**, 1091–1110.
White, J. C. & Flagler, P. A. 1992. Deformation within part of a major crustal shear zone, Parry Sound, Ontario: structure and kinematics. *Can. J. Earth Sci.* **29**, 129–141.
White, J. C. & Mawer, C. K. 1992. Deep-crustal deformation textures along megathrusts from Newfoundland and Ontario: implications for microstructural preservation, strain rates, and strength of the lithosphere. *Can. J. Earth Sci.* **29**, 328–337.
White, S. H. 1979. Large strain deformation: report on a Tectonic Studies Group discussion meeting held at Imperial College, London. *J. Struct. Geol.* **1**, 333–339.
White, S. H., Burrows, S. E., Carreras, J., Shaw, N. D. & Humphreys, F. J. 1980. On mylonites in ductile shear zones. *J. Struct. Geol.* **2**, 175–187.
Williams, P. F. 1985. Multiply deformed terrains: problem of correlation. *J. Struct. Geol.* **7**, 269–280.
Williams, P. F. & Price, G. P. 1990. Origin of kinkbands and shear-band cleavage in shear zones: an experimental study. *J. Struct. Geol.* **12**, 145–164.
Wood, D. S. 1973. Patterns and magnitudes of natural strain in rocks. *Trans. R. Soc. Lond.* **A274**, 373–382.
Zwart, H. J. 1960. Relations between folding and metamorphism in the Pyrenees and their chronological succession. *Geologie Mijnb.* **39e**, 163–180.

## APPENDIX

*Velocity field of two-slip-system accommodated flows*

We set a reference frame ($xy$) with one slip system ($\dot{\gamma}_1$, Fig. A1) parallel to the $x$-axis. The other slip system makes an arbitrary angle $\theta$ with respect to $x$. The Eulerian velocity at an arbitrary point P is the sum of two components contributed by $\dot{\gamma}_1$ and $\dot{\gamma}_2$, respectively.

The velocity component as a result of $\dot{\gamma}_1$ is:

$$\begin{bmatrix} u_1 \\ v_1 \end{bmatrix} = \begin{bmatrix} 0 & \dot{\gamma}_1 \\ 0 & 0 \end{bmatrix} \begin{bmatrix} x \\ y \end{bmatrix}. \qquad \text{(A1)}$$

The velocity component as a result of $\dot{\gamma}_2$ is, expressd in $x_1y_1$:

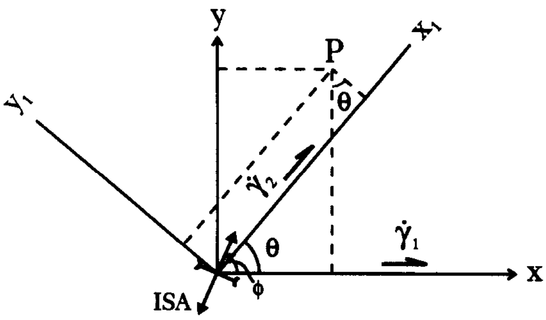


Fig. A1. Reference frame for the derivation of the flow velocity field for two-slip-system-accommodated flow. $x$ ($\dot{\gamma}_1$) and $x_1$ ($\dot{\gamma}_2$) are orientations of the two slip systems and the accommodating shear strain rates. P is an arbitrary point. The maximum principal stretching axis make an angle $\phi$ with respect to the $x$-axis (one slip system). See text for details.

$$\begin{bmatrix} u_2 \\ v_2 \end{bmatrix} = \begin{bmatrix} 0 & \dot{\gamma}_2 \\ 0 & 0 \end{bmatrix} \begin{bmatrix} x_1 \\ y_1 \end{bmatrix}. \quad \text{(A2)}$$

Since the transformation from $x_1y_1$ to $xy$ is:

$$\begin{bmatrix} x_1 \\ y_1 \end{bmatrix} = R \begin{bmatrix} \cos\theta & \sin\theta \\ -\sin\theta & \cos\theta \end{bmatrix} \begin{bmatrix} x \\ y \end{bmatrix}, \quad \text{(A3)}$$

A2 when transformed into the $xy$ frame, becomes:

$$\begin{bmatrix} u_2 \\ v_2 \end{bmatrix} = R^T \begin{bmatrix} 0 & \dot{\gamma}_2 \\ 0 & 0 \end{bmatrix} R = \begin{bmatrix} -\dot{\gamma}_2 \sin\theta\cos\theta & \dot{\gamma}_2 \cos^2\theta \\ -\dot{\gamma}_2 \sin^2\theta & \dot{\gamma}_2 \sin\theta\cos\theta \end{bmatrix} \begin{bmatrix} x \\ y \end{bmatrix} \quad \text{(A4)}$$

Therefore, the Eulerian velocity field, being the sum of two components, is:

$$\begin{bmatrix} u \\ v \end{bmatrix} = \begin{bmatrix} u_1+u_2 \\ v_1+v_2 \end{bmatrix} = \begin{bmatrix} -\dot{\gamma}_2 \sin\theta\cos\theta & \dot{\gamma}_1+\dot{\gamma}_2\cos^2\theta \\ -\dot{\gamma}_2 \sin^2\theta & \dot{\gamma}_2 \sin\theta\cos\theta \end{bmatrix} \quad \text{(A5)}$$

The velocity gradient tensor **L** is:

$$\mathbf{L} = \begin{bmatrix} -\dot{\gamma}_2 \sin\theta\cos\theta & \dot{\gamma}_1+\dot{\gamma}_2\cos^2\theta \\ -\dot{\gamma}_2 \sin^2\theta & \dot{\gamma}_2 \sin\theta\cos\theta \end{bmatrix}. \quad \text{(A6)}$$

From A6, the stretching tensor **D** and vorticity tensor **W** can be easily obtained (see Means *et al.* 1980):

$$\mathbf{D} = \begin{bmatrix} -\frac{1}{2}\dot{\gamma}_2 \sin 2\theta & \frac{\dot{\gamma}_1+\dot{\gamma}_2\cos 2\theta}{2} \\ \frac{\dot{\gamma}_1+\dot{\gamma}_2\cos 2\theta}{2} & \frac{1}{2}\dot{\gamma}_2 \sin 2\theta \end{bmatrix}$$

$$\mathbf{W} = \begin{bmatrix} 0 & \frac{\dot{\gamma}_1+\dot{\gamma}_2}{2} \\ -\frac{\dot{\gamma}_1+\dot{\gamma}_2}{2} & 0 \end{bmatrix} \quad \text{(A7)}$$

The principal stretching rates are the two eigenvalues of **D** and the eigenvectors of **D** are the orientations of the ISA. The maximum stretching axis makes an angle $\phi$ with respect to the $x$-axis:

$$\phi = \tan^{-1}\frac{\sin 2\theta + (1 + C^2 + 2C\cos 2\theta)^{1/2}}{C + \cos 2\theta}, \quad \text{(A8)}$$

where $C = \dot{\gamma}_1/\dot{\gamma}_2$.

The vorticity of the flow is $\dot{\gamma}_1 + \dot{\gamma}_2$. The spin component of the vorticity is:

$$\text{spin} = W_S = -2\frac{d\phi}{dt} = -2\frac{d\phi}{dC}\frac{dC}{dt}. \quad \text{(A9)}$$

The negative sign represents that a decrease of $\phi$ corresponds to the sympathetic sense of spin. If during the development of the shear bands, the shear strain rate ratio $C$ is taken to be nearly constant, the spin is then negligible. In such a case, the non-coaxiality of the flow is:

$$W'_k = \frac{1 + C}{(1 + C^2 + 2C\cos 2\theta)^{1/2}}. \quad \text{(A10)}$$

Since $(1 + C^2 + 2C\cos 2\theta)^{1/2} \leq 1 + C$, it is clear that $W'_k$ is always greater than unity, i.e. the flow is super-simple shear. From field observation, the two sets of shear bands are equally developed, suggesting $C \approx 1$, and the angle $\theta = 55°$. This gives an estimated non-coaxiality of 1.74.